Journal of Engg. Research Vol. 6 No. (3) September 2018 pp 225-241

Characterization of the dynamic heterogeneity during polymer flooding in reservoirs with stratified non-communicating layers

Yongge Liu*,**, Jian Hou*,**, Jingyao Liu*,**, Qing Wang*** and Kai Dong ****

** State Key Laboratory of Heavy Oil Processing, China University of Petroleum, Qingdao, Shandong 266580, China*

*** School of Petroleum Engineering, China University of Petroleum, Qingdao, Shandong 266580, China*

**** School of Petroleum Engineering, China University of Petroleum, Beijing, China*

***** Baker Hughes, Houston, TX, USA*

** Corresponding Author: houjian@upc.edu.cn (J. Hou)*

ABSTRACT

Heterogeneity affects the development performance greatly and, therefore, is an important property of the reservoir. The conventional method mainly takes permeability, which often does not change during the production process as the characterization parameter of heterogeneity. However, in polymer flooding, the injected polymer is more likely to enter the high-permeability zone with low resistance, which leads to the decrease of the resistance difference between the high and low-permeability zones. This non-uniform resistance due to the unbalanced distribution of polymer solution changes the heterogeneity of the reservoir dynamically, and it cannot be reflected by the current representation method. In this paper, a new parameter called "motivation coefficient" (I_P) is proposed, in which not only is the static permeability included, but also the dynamic parameters related with polymer property are taken into consideration, and the Gini coefficient of I_P ($\boldsymbol{GC_{IP}}$) is selected to represent the dynamic heterogeneity during polymer flooding. Then physical experiment and numerical simulations are done to study the variation law of dynamic heterogeneity during the polymer flooding. The results show that the dynamic heterogeneity is greatly improved after polymer injection. However, at the subsequent water flooding stage, the dynamic heterogeneity is more intensified when the whole polymer flooding process is over. Comprehensively considering the dynamic heterogeneity and development performance, the most favorable value of Gini coefficient of permeability is 0.6, and the best range of polymer concentration is from 0.1% to 0.15%. As for the slug size, large sizes are preferred if they are economically viable.

Keywords: dynamic heterogeneity; quantitative characterization; polymer flooding; Lorenz curve.

INTRODUCTION

Heterogeneity denotes the non-uniform distribution of reservoir properties. Strong reservoir heterogeneity will lead to short water breakthrough time and low swept volume and, therefore, bring down the final oil recovery. Representation of reservoir heterogeneity is of great importance to the reservoir development, and, by far, many representation methods have been proposed. Dykstra and Parson (1950) defined a parameter V_{dp} and through matching to permeability distribution of the reservoir, the formula of V_{dp} was obtained. Now V_{dp} has become one of most popular parameters to represent reservoir heterogeneity. Based on V_{dp}, Moissis and Wheeler (1990) proposed a parameter named permeability variation coefficient (the ratio of variance to expectation) to characterize the reservoir heterogeneity. According to the streamline simulation results, Shook et al. (2009) proposed a dynamic Lorenz coefficient and find that it was robust to rank the heterogeneity of various geological models. Liu et al. (2017) proposed a parameter that considered relative permeability and investigated the dynamic heterogeneity during water flooding.

Polymer flooding is the most widely used chemical flooding method in the world, and industrial tests of polymer flooding have been successfully conducted in Canada, France, Germany, Oman, China, and so on (Wang et al., 1994; Niu, 2004; Wang et al., 2005; Li et al., 2016; Hernandez, et al., 2003; Carrero, et al., 2007; Lv et al., 2015; Chen et al., 2015). Along with the wide spread filed application, many scholars devoted themselves to the researches of polymer flooding mechanisms. Needham and Doe (1987) found that polymers can significantly reduce water relative permeability in the swept zone and, thus, enhance oil recovery greatly. By physical experiments, Hird and Dubrule (1998), You (2009), Gharbi (2001), and Alsofi and Blunt (2010) found that, after long-term water flooding, the resistance in high- and low-permeability zones can differ in dozens or even hundreds of times. However, when the polymer solution is injected, the water-oil mobility ratio is effectively reduced because of the viscosifying action of the polymer solution. Hence, the viscous fingering subsides, the swept volume expands, and the oil recovery increases. By microscopic visual experimental research, Wang et al. (2000) found that polymer not only can enlarge the sweep efficiency, but also can enhance the displacement efficiency due to its viscoelastic property. The investigation results of Wu et al. (2006) and Cheng et al. (2010) showed that when the polymer flows through the porous media, it can be retained by means of adsorption and capture. The retained polymer induces a certain resistance to the following injected water, which, to some extent, also increases the swept volume of the following water injection. Wang and Dong (2009) found that the polymer adsorption tends to narrow the water flow channels, and thus the following polymer solution and water will be diverted to flow in the oil flow channel. By numerical simulation, Shi et al. (2010) found that high residual resistance factor is preferable to enhance oil recovery due to the high resistance in the high-permeability zone caused by the retained polymer at the subsequent water flooding period. Khorsandi et al. (2016) investigated the development performance of low salinity polymer flooding, and the results showed that the low salinity water can keep the polymer solution's viscosity at a high level, and therefore a good performance can be achieved.

It can be seen from the above analysis that the polymer solution is not uniformly distributed in the reservoir after polymer injection and due to the high viscosity of the polymer solution and the residual resistance of the adsorbing polymer, the resistance between the high- and low-permeability zones will be changed. Therefore, the heterogeneity of polymer flooding shows dynamic properties. Although there have been many studies on representation methods of heterogeneity by far, most of these researches take permeability, which often does not change during the production process as the characterization parameter. Studies on the changing law of dynamic heterogeneity and its quantitative characterization are rare. In order to investigate the dynamic changes of heterogeneity during polymer flooding process, a new parameter called "motivation coefficient" (I_P) is proposed, in which not only is the static permeability included, but also the dynamic parameters related with the polymer property are taken into consideration, and the Gini coefficient of I_P (GC_{IP}) is selected to represent the dynamic heterogeneity during polymer flooding. Then physical experiment and numerical simulations are conducted, and the variation law of dynamic heterogeneity is investigated.

SELECTION OF A CHARACTERIZING PARAMETER

Taking an element with size $\Delta x\times\Delta y\times\Delta z$ as the research object, if the capillary pressure is neglected, then the total fluid velocity at x direction during the polymer flooding process is obtained as follows:

$$v_x = \frac{\dfrac{\Delta\Phi_x}{\mu_o \Delta x}}{k_x(k_{ro} + \dfrac{\mu_{rp}k_{rw}}{R_k})} \tag{1}$$

where v is the total fluid velocity, m/s; $\Delta\Phi$ is the potential energy, Pa; μ_o and μ_{rp} are oil viscosity and polymer viscosity, respectively, Pa.s; Δx is the length of the element, m; k is the absolute permeability, m^2; k_{rw} and k_{ro} are water and oil relative permeability, respectively; R_k is the residual resistance factor; x is the direction.

Therefore, the fluid flow rate at *x, y* and z direction should be

$$Q_x = \frac{\dfrac{\Delta\Phi_x}{\mu_o \Delta x}}{k_x(k_{ro} + \dfrac{\mu_{rp}k_{rw}}{R_k})}\Delta y\Delta z \tag{2}$$

$$Q_y = \frac{\dfrac{\Delta\Phi_y}{\mu_o \Delta y}}{k_y(k_{ro} + \dfrac{\mu_{rp}k_{rw}}{R_k})}\Delta x\Delta z \tag{3}$$

$$Q_z = \frac{\dfrac{\Delta\Phi_z}{\mu_o \Delta z}}{k_z(k_{ro} + \dfrac{\mu_{rp}k_{rw}}{R_k})}\Delta x\Delta y \tag{4}$$

where Q is the flow rate, m^3/s; *y* and *z* are the directions.

We assume that the permeability at y direction is equal to that at *x* direction, and the vertical permeability is proportional to the plane permeability, that is, $k_x=k_y=\alpha k_z$ (α is constant). Also we assume that $\Delta x = \beta\Delta y = \gamma\Delta z$ (β and γ are constants); then the total flow rate of the flux should be

$$Q_t = Q_x + Q_y + Q_z = \frac{\dfrac{\Delta\Phi_x + \beta\Delta\Phi_y + \eta\Delta\Phi_z}{\mu_o}}{k(k_{ro} + \dfrac{\mu_{rp}k_{rw}}{R_k})\Delta x} \tag{5}$$

where Q_t is the total flow rate, m^3/s; $\eta=\gamma/\alpha$.

From Eq. (5), we can see that the numerator is the combination of the potential energies, and it can be seen as the driving force of oil and water flow. Then the denominator can be seen as the resistance, and we denote the resistance as R_P. R_P not only reflects the static properties including permeability and fluid viscosity, but also considers dynamic parameters including relative permeability. Moreover, the viscosity of the polymer solution and residual resistance factor are also included in the formula of RP. So R_P can not only represent the heterogeneity of permeability, but also reflect the dynamic heterogeneity during polymer flooding. Notice that, in Eq. (5), k is in the denominator, and it mainly takes permeability as the characterizing parameter at present (Dykstra and Parson, 1950; Mossis and Wheeler, 1990; Zhou, 1997; Henson, 2002). So, in order to keep a similar type with most of the present methods, we define a new parameter named motivation factor (I_P) with expression as follows:

$$I_P = \frac{1}{R_P} = \frac{k}{\dfrac{\mu_o}{\left(k_{ro} + \dfrac{\mu_{rp} k_{rw}}{R_k}\right)\Delta x}} \tag{6}$$

where R_P is the resistance, Pa/(m^3/s); I_P is the motivation factor, (m^3/s)/Pa.

From Eq. (6), we can conclude that if the field only has one relative permeability curve, then the difference of I_P only reflects that of the permeability before water flooding and in this situation, taking I_P or the permeability to characterize heterogeneity will obtain the same result. However, when the production begins, the water saturation of the elements will differ and I_P will show its dynamic properties. If polymer flooding is conducted, the non-uniform distribution of polymer solution in the reservoir also affects the dynamic heterogeneity, and this is an ever-changing process. By analyzing the variation law of I_P, the regularity of dynamic heterogeneity during polymer flooding can be obtained.

If the target of the research is paralleled cores, the length of each core is short and we can treat it as a whole. Then the total resistance of an individual core is

$$R_P = -\int_0^L \frac{\mu_o}{kA(k_{ro} + \dfrac{\mu_{rp} k_{rw}}{R_k})} dx \tag{7}$$

where A is the sectional area, m^2.

So, the formula of I_P of each core should be

$$I_P = \frac{1}{R_P} = -\frac{k}{\displaystyle\int_0^L \frac{\mu_o}{A(k_{ro} + \dfrac{\mu_{rp} k_{rw}}{R_k})} dx} \tag{8}$$

PHYSICAL EXPERIMENTS

From Eq. (2) to (8), for each core, we can get

$$I_P = \frac{Q_t}{\Delta\Phi} \tag{9}$$

For parallel connected cores, the differential pressures of the cores are the same. Therefore, from Eq. 9, I_p has a linear relationship with Q_t , which can be recorded easily by experiment. Due to this, the following experiment is designed to study the influence of polymers on dynamic heterogeneity.

The schematic plot of the five parallel sandpacks' polymer flooding experiment is shown in Fig. 1. The equipment mainly consists of five parts, such as the injection system, five paralleled sandpacks, data acquisition system, production system, and auxiliary system. The injection system is mainly composed of an injection pump and three containers with oil, formation water, and polymer solution, respectively, with which the simultaneous injection of water and polymer solution can be easily operated. The salinity of the formation water is 10129mg/L. The data acquisition system consists of a computer, a data collector, and some pressure sensors, and the function of this system is to implement real-time pressure data collection. The production system is mainly composed of a series of controlled valves and volumetric cylinders, and the main function is to precisely measure the volume of oil and water produced. The auxiliary system mainly consists of a thermostat and a drying oven. When the experiment begins, the water will be injected into the containers under the driving force supported by the pump, and the oil, water, or polymer in the containers will flow into the sandpacks through the valve. Then the produced water and oil will be collected by the volumetric cylinders, and the pressures during the flooding process will be measured by the pressure sensors and then recorded by the computer.

Experimental apparatus and procedures

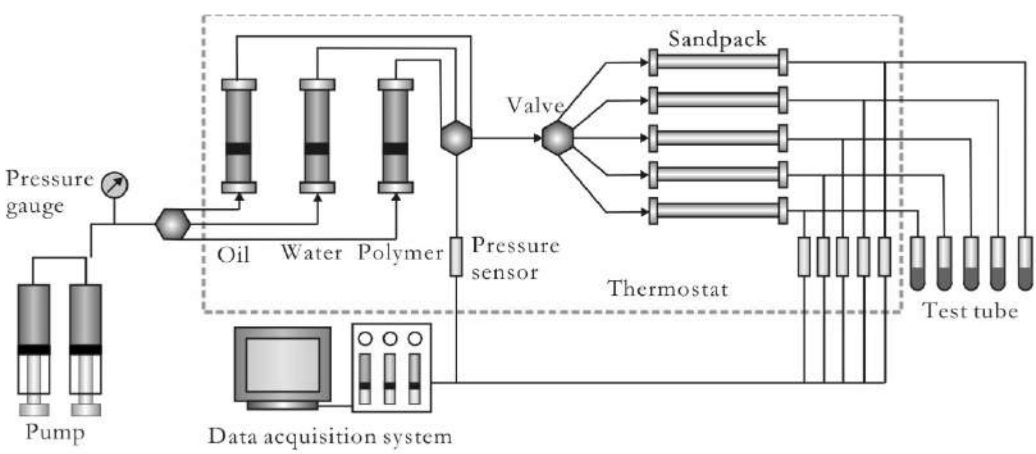

Fig. 1. Experimental apparatus.

The experimental steps are as follows:

(1) The five sandpacks were filled by quartz sands with mesh numbers from 60 to 160, respectively, to obtain the heterogeneity of permeability.

(2) The sandpacks were vacuumized and saturated by water. The porosity of each sandpack was calculated by the volume of water saturated, and the permeability was calculated by the pressure drop according to Darcy's law.

(3) All the apparatuses were assembled according to Fig. 1, and the temperature of the thermostat was set to 65 °C.

(4) The five parallel sandpacks were water-flooded with a water injection rate of 5mL/min and when the watercut reaches 98%, a polymer slug is injected with an injection rate of 5mL/min. The mass concentration of the polymer slug is 0.1%, and the slug size is 0.2PV.

(6) The five parallel sandpacks were water-flooded again at a rate of 5mL/min and when the watercut was 98%, the whole experiment was finished.

Result analysis

The key parameters of sandpacks, oil, and polymer are listed in Tables 1 and 2, respectively.

Table 1. Properties of sandpacks.

No.	Length cm	Diameter cm	Porosity %	Permeability mD
1	30	3.8	32.6	2384
2	30	3.8	31.8	1197
3	30	3.8	32.2	632
4	30	3.8	30.9	488
5	30	3.8	33.4	364

Table 2. Basic fluid properties.

Oil viscosity mPa.s	Polymer type	Polymer viscosity 10s-1
23.6	KY-II	(0.05%) 5.9
		(0.1%) 24.9
		(0.15%) 51.9
		(0.2%) 85.3

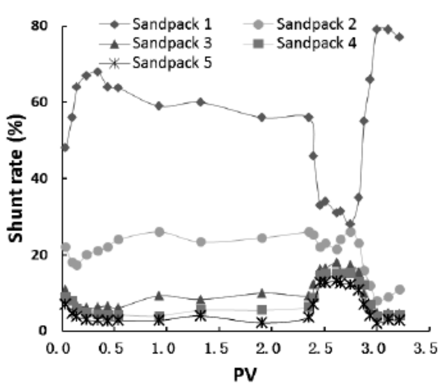

(a) Shunt rate curves

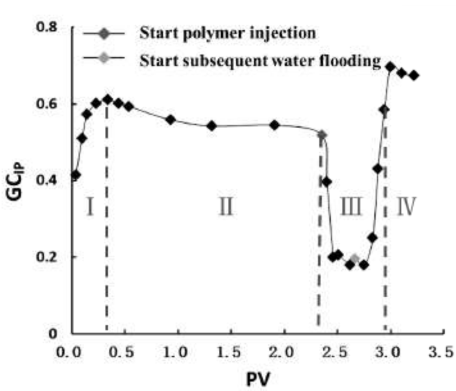

(b) GC_{IP} curves

Fig. 2. Curves of shunt rate and GCIP.

Eq. (9) indicates that the differences of shunt rate (percentage of the individual flow rate to the total flow rate) at different times reflect the differences of I_P. In this paper, the Lorentz curve method was used to describe the change of dynamic heterogeneity during polymer flooding, where the I_P values of the five cores were used to generate the Lorentz curve and the Gini coefficient (abbr. GC_{IP}, dimensionless), which is calculated according to Lorentz curve that was used as the criterion to evaluate the dynamic heterogeneity (Shook and Mitchell, 2009; Wang et al., 2010).

Fig. 2 (a) shows the changing curves of the shunt rate of each sandpack along with the times of the injected pore volume of water (PV, dimensionless). According to the data in Fig. 2(a), the changing curve of GC_{IP} in the whole flooding process is calculated and shown in Fig. 2(b). It can be seen from the figures that the GC_{IP} curve can be divided into four stages denoted by I, II, III, and IV. In stage I, GC_{IP} increases sharply, which means that the dynamic heterogeneity is greatly intensified. This is because the shunt rate of sandpack 1 is the highest due to its high permeability. Moreover, as the production of viscous oil goes on, its resistance reduces rapidly and I_P grows sharply on the contrary. However, the resistance in other sandpacks decreases slowly due to the low initial shunt rates. So, the differences in I_P between sandpack 1 and other sandpacks grow and GC_{IP} increases at a fast rate. In stage II, GC_{IP} decreases slowly, which means that the dynamic heterogeneity is slightly weakened. This is because, after water breakthrough of the sandpack 1, its watercut increases gradually and the change of its resistance slows down at high watercut stage. However, for other sandpacks, the watercuts are at a low level or even 0. As the production goes on, the resistance decreases at a relatively high rate and the difference in I_P between sandpack 1 and other sandpacks decreases slowly. In stage III, the polymer solution is injected into the sandpacks. GC_{IP} keeps a low value at this stage, which means that the dynamic heterogeneity is greatly improved after polymer injection. This is because, the same as stage I, the polymer solution flows more into sandpack 1 with the highest permeability and the least resistance. Due to the high viscosity and residual resistance of the polymer solution, the resistance of sandpack 1 increases sharply. However, the resistance increase of other sandpacks is relatively small due to the low shunt rates, and the difference of I_P between high- and low-permeability sandpacks is reduced. So, GC_{IP} decreases to a low value in a short time and the shunt rate of each sandpack tends to be equal leading to an increase of swept volume. In stage IV, GC_{IP} increases sharply again, and it even goes beyond that before polymer flooding, which means that the dynamic heterogeneity is more intensified when the whole polymer flooding process is over. This is because the polymer solution in sandpack 1 is first produced due to its highest shunt rate. So the corresponding resistance decreases sharply, and the value of I_P grows rapidly. In contrast, the polymer solution in low-permeability sandpacks is produced slowly or even hardly due to the low shunt rates, and this part of polymer exerts great resistance to the low-permeability sandpacks. Hence, the difference in I_P of high- and low-permeability sandpacks rises significantly, which can be more severe than that before polymer flooding. The experimental results have shown that the oil recovery of water flooding is 40.5%, and polymer flooding can increase the oil recovery by 8.2%. This means that there is still 51.3% oil unswept after polymer flooding. However, due to the much intensified dynamic heterogeneity, after polymer flooding, it is much more difficult to further enhance oil recovery.

Numerical simulation

The experiment is often tedious and time-consuming. Therefore, in this part, a numerical simulation model is built, and then history matching is done based on the experimental results. Finally, the variation law and influencing factors of dynamic heterogeneity are investigated.

History matching

The numerical simulation model of polymer flooding on five parallel sandpacks was established using STARS module of commercial software CMG. The length, sectional area, porosity, and permeability of each sandpack were defined according to Table 1, and the relative permeability curve of each sandpack was defined according to Stone model:

$$k_{ro} = k_{rocw}\left(\frac{1-S_w-S_{or}}{1-S_{wc}-S_{or}}\right)^{n_o} \qquad k_{rw} = k_{rwro}\left(\frac{S_w-S_{wc}}{1-S_{wc}-S_{or}}\right)^{n_w} \tag{10}$$

where S_{wc} and S_{or} are irreducible water saturation and residual oil saturation, respectively; k_{rocw} and k_{rwro} are oil relative permeability at S_{wc} and water relative permeability at S_{or}, respectively; k_{rwro} is the water relative permeability at residual oil saturation; n_o and n_w are exponents.

Table 3. Parameters in Stone model.

No.	1	2	3	4	5
S_{wc}	0.29	0.32	0.29	0.31	0.33
S_{or}	0.28	0.28	0.29	0.30	0.32
k_{rocw}	1	1	1	1	1
k_{rwro}	0.63	0.58	0.52	0.54	0.6
n_o	1.8	2.1	1.9	2.2	2.9
n_w	2.3	2.1	2.0	2.6	3.2

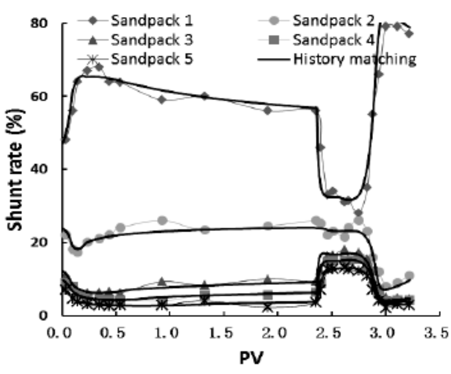

Fig. 3. History matching.

Table 4. Keywords and values in the simulation model.

Mechanisms	Keywords	Values	Unit
Composition-dependent viscosity effects	*AVISC	85.3	mPa.s
	*BVISC	0	°C
	*VSMIXENDP	0.0020	Dimensionless
	*VSMIXFUNC	Sub-Table 4(1)	Dimensionless
Polymer adsorption	*ADSTABLE	Sub-Table 4(2)	Dimensionless
	*ADMAXT	0.42	kg/m³
	*ADRT	0	kg/m³
Permeability reduction	*RRFT	2.0	Dimensionless
Inaccessible pore volume	*PORFT	0.9	Dimensionless
Sub-Table 4(1) mixing function		**Sub-Table 4(2) Adsorption table**	
Polymer concentration (mg/L)	Mixing function	Polymer concentration (mg/L)	Adsorbed mass (kg/m²)
0	0.00	0	0
250	0.16	500	0.19
500	0.40	1000	0.39
750	0.61	1500	0.41
1000	0.72	2000	0.42
1250	0.81		
1500	0.89		
1750	0.95		
2000	1.00		

The history matching of water flooding period was conducted by adjusting the parameters in Eq. (10). Table 3 shows the key parameters of the relative permeability of the five sandpacks after history matching. In Table 3, S_{wc} was calculated according to the volumes of water and oil saturated, and S_{or} was calculated by the volumes of oil saturated and produced in the experiment. k_{rocw} is always 1 in Stone model. k_{rwro}, no and nw were obtained according to history matching of the experimental results of water flooding period. The history matching of polymer flooding period was achieved by adjusting the viscosity-concentration relationship of polymer solution, residual resistance factor, and other parameters. Table 4 shows the polymer properties used in numerical simulation after history matching. Fig. 3 shows the history matching result of the shunt rates.

Analysis on changing law of IP in polymer flooding

Fig. 4 shows the IP distribution of each grid in different development stages, which also was obtained by STARS module. The sandpack number increases in turn from bottom to top; that is, the permeability of the sandpack at the bottom is the highest. The right side is the injection end, and the left, the production end. In order to compare the relative magnitude of I_P in all stages, all the values of I_P have been transformed into dimensionless variations with the least I_P value among all grids used as the standard value. It is shown by the figure that, initially, the disparity of I_P is only induced by the permeability difference, and hence I_P is equal everywhere within each sandpack (Fig. 4(a)). After water flooding starts, the injected water flows more into the sandpacks with high permeability, and the resistance of the high-permeability sandpack decreases with the production of viscous oil, which leads to the increase of I_P. However, I_P of the low-permeability sandpack only decreases slightly. So, the gap of I_P between the sandpacks is enlarged, and the dynamic heterogeneity is intensified (Fig. 4(b)). When polymer injection starts, the polymer solution also tends to enter the high-permeability sandpack with the least resistance. Due to the high viscosity and residual resistance of the polymer solution, the resistance near the injection end rises sharply and I_P drops correspondingly. So the dynamic heterogeneity is improved greatly, and the shunt rates of sandpacks tend to be equal (Fig. 4(c) and Fig. 4(d)). Although the differences among the shunt rates are much reduced, the shunt rate in the high-permeability sandpack remains the highest. Hence, the polymer solution in the high-permeability sandpack is first produced in the following water flooding stage, which causes a rapid increase of I_P in the sandpack. On the contrary, the polymer solution in medium- and low-permeability sandpacks is slowly or hardly produced, and this part of polymer exerts great resistance to these sandpacks. So the I_P gap between high- and low-permeability sandpacks increases quickly and even goes beyond the value before polymer flooding. The dynamic heterogeneity becomes much severer, and further enhancing oil recovery becomes much more difficult (Fig. 4(e), Fig. 4(f)).

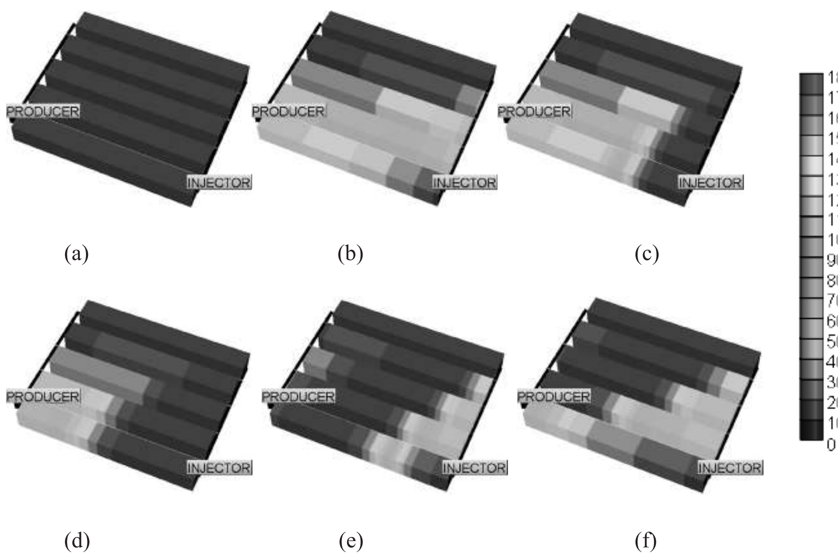

Fig. 4. Distribution of dimensionless IP at different times: (a) initial time; (b) watercut equals 98%; (c) polymer injection for 0.1PV; (d) polymer injection for 0.2PV; (e) subsequent water flooding for 0.2PV; (f) subsequent water flooding for 0.4PV.

Analysis of influencing factors of dynamic heterogeneity in polymer flooding

According to Fig. 2(b), the general variation curve of GC_{IP} is shown in Fig. 5. The variation law of dynamic heterogeneity in polymer flooding differs from that of the general water flooding only in the polymer injection stage and the subsequent water flooding stage. Hence, in this paper, the area of the shape ABCD, which was denoted by S_P, was defined as the evaluation index of the improvement of dynamic heterogeneity by polymer flooding, and the difference between the GC_{IP} values at the points E and F, which was denoted by GC_{EF}, was used to assess the final influence of polymer flooding on dynamic heterogeneity when the whole polymer flooding process is over.

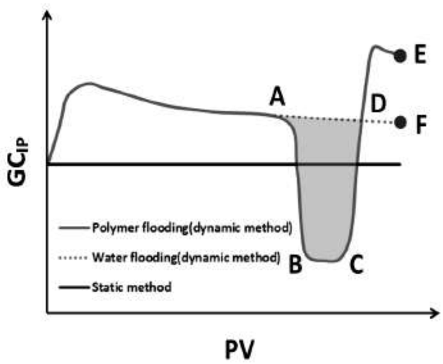

Fig. 5. Schematic of the changing law of GC_{IP}.

Effects of permeability heterogeneity on dynamic heterogeneity in polymer flooding

Wang (2013) used a series of functions to match the shape of Lorenz curves and built a method to obtain the permeability distribution with a certain Gini coefficient. By his method, the permeability distributions with the Gini coefficient of 0.2, 0.4, 0.6, and 0.8 are calculated and shown in Table 5.

Table 5. Permeability distributions with different GC_P.

GC_P	Sandpack 1	Sandpack 2	Sandpack 3	Sandpack 4	Sandpack 5
0.2	4.570	3.542	2.524	2.162	1.812
0.4	6.907	3.477	1.782	1.409	1.034
0.6	10.256	1.969	1.110	0.795	0.479
0.8	12.951	0.661	0.497	0.333	0.169

The average permeability of all cases is 1013 mD, which is the same as that in the physical experiment. Four cases were all simulated, and the curves of GC_{IP} in polymer injection and the subsequent water flooding stage are shown in Fig. 6. It can be seen from Fig. 6(a) that, with the increase in the permeability Gini coefficient (abbr. GC_P), GC_{IP} starts to rise early. This is because, at the subsequent water flooding stage, the sandpack with high-permeability gains higher shunt rate and the polymer solution is firstly produced, which leads to a sharp increase of I_P. So, at this time, the resistance gap between high- and low-permeability sandpack becomes increasing, and GC_{IP} also increases correspondingly. When GC_P is low, the difference of shunt rates is relatively small, so that it needs a long time to flood the polymer out. On the contrary, when GC_P is high, the polymer solution in the sandpack with high permeability is produced in a short time, and the resistance gap between high- and low-permeability sandpacks increases sharply leading to a rapid growth of GC_{IP}. Fig. 6(b) compares S_P and GC_{EF} with different GC_P values. It has been shown that S_P first increases and then drops, reaching the highest when GC_P is 0.6. This is because low GC_P indicates low-permeability heterogeneity among sandpacks. Water flooding is sufficient to achieve the desired development performance, and the improvement of the dynamic heterogeneity by polymer injection is limited in such condition. When GC_P is too high, although GC_P drops greatly, it starts to increase early and SP is also relatively small. The comparison of GC_{EF} shows that GC_{EF} decreases rapidly with the increase in GC_P. When GC_P is 0.8, GC_{EF} is almost negligible. This is because when the GC_P is relatively small, the amount of polymer injected into the medium- and low-permeability sandpacks in polymer flooding is relatively high, and hence the resistance induced by polymer retained in the sandpacks is large. So, with the polymer solution in the high-permeability sandpack produced in the subsequent water flooding stage, GC_{IP} increases significantly. Combining Fig. 6(a) and Fig. 6(b), we can see that when GC_P is 0.6, S_P is the highest and GC_{EF} is relatively small, which indicates that 0.6 is the most favorable value of GC_P for polymer flooding.

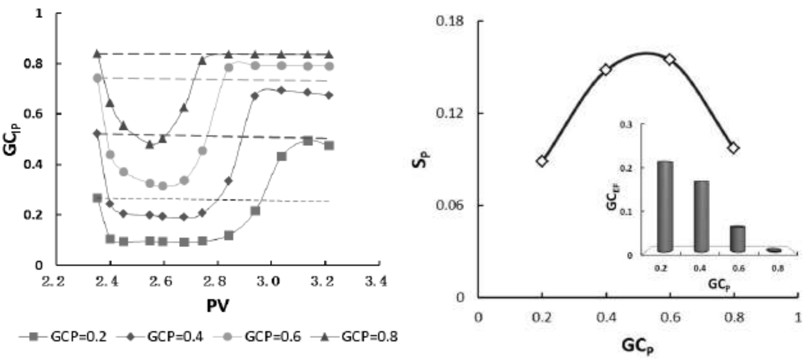

(a) Curves of GC_{IP} (b) Curves of S_P & GC_{EF}

Fig. 6. Effect of permeability heterogeneity on dynamic heterogeneity.

Effects of polymer concentration on dynamic heterogeneity in polymer flooding

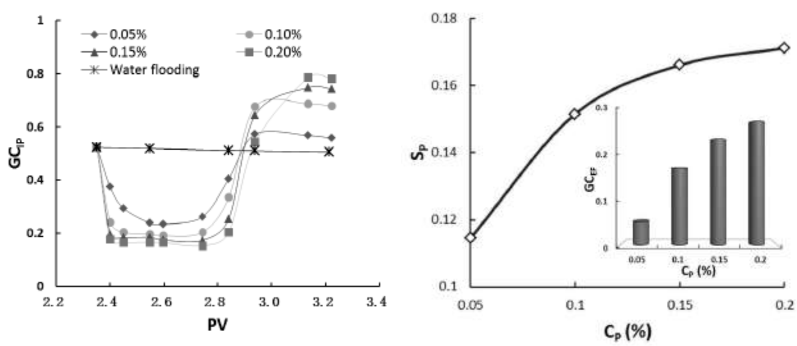

(a) Curves of GC_{IP} (b) Curves of S_P & GC_{EF}

Fig. 7. Effect of polymer concentration on dynamic heterogeneity.

The permeability of the sandpacks is set according to the experiment. The cases with polymer concentrations of 0.05%, 0.1%, 0.15%, and 0.2% are simulated, respectively. The changing curve of GC_{IP} is shown in Fig. 7(a), and SP and GC_{EF}, under different polymer concentrations, are calculated according to Fig. 7(a), shown in Fig. 7(b). From this figure, we can see that as the polymer concentration increases, GC_{IP} reduces faster and the minimum value becomes smaller. The reason is that the polymer first enters the high-permeability sandpack when polymer flooding begins, which causes the increase of resistance in high-permeability sandpack and decrease of GC_{IP}. The higher the polymer concentration is, the faster the I_P value of high-permeability core is reduced, and the earlier the GC_{IP} reaches its lowest value. However, from the viscosity-concentration relationship of the polymer solution, we can see that when the polymer concentration is 0.1%, the viscosity of the polymer solution is nearly equal to that of the oil and the performance of the polymer solution on profile control is good enough. Continuing increasing the polymer concentration can no longer achieve notable improvement. So, S_P increases constantly as the polymer concentration rises, but the amplitude of the increase is small with the concentration beyond 0.1%. Moreover, as the polymer concentration increases, GC_{EF} grows continuously. This is because the bigger the polymer concentration leads to larger resistance when the polymer is injected, the bigger the I_P difference is after the production of polymer in sandpack with high permeability. Combining Figs. 7(a) and 7(b), we can conclude that polymer concentration from 0.1% to 0.15% is the most favorable value for polymer flooding.

Effects of polymer slug size on dynamic heterogeneity in polymer flooding

The cases with polymer slug sizes of 0.2PV, 0.4PV, 0.6PV, and 0.8PV are simulated, respectively, and the corresponding changing curve is shown in Fig. 8. It is shown that the GC_{IP} does not decrease as the slug size increases, and the corresponding lowest GC_{IP} to each slug size is the same, which indicates that larger polymer slug size will not improve the dynamic heterogeneity to a lower level. However, with the increase in slug size, GC_{IP} stays at a low value for a longer time. So large-size slugs extend the time during which the dynamic heterogeneity remains at a relatively low level, and hence it helps the development of low-permeability zones and enhancement of the sweep efficiency. From the S_P changing curve, the relation between SP and the slug size is nearly linear, which is totally different from that between SP and the polymer concentration shown in Fig. 7(b). From the comparison of GC_{EF} , we can see that GC_{EF} increases gradually with the increase in the slug size of polymer solution.

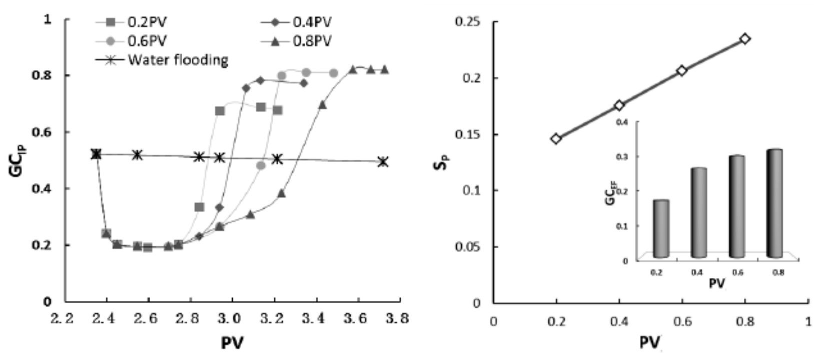

(a) Curves of GC_{IP} (b) Curves of SP & GC_{EF}

Fig. 8. Effect of polymer slug size on dynamic heterogeneity.

This is because the time during which the dynamic heterogeneity remains low is extended due to the large-size slug; the polymer solution that flows into medium- and low-permeability zones increases during polymer injection. With the polymer solution of high-permeability zones being produced continuously in the subsequent water flooding stage, the large size slug will cause high GC_{EF}, because the polymer solution retained in low-permeability zones has grown. However, from the changing curve of GC_{EF}, when the slug size is beyond 0.4PV, the increase magnitude of GC_{EF} significantly decreases. Comprehensively considering the changing law of S_P and GC_{EF}, it is safe to say that large-size slugs can effectively extend the period within which the dynamic heterogeneity remains relatively low and meanwhile avoid increasing the dynamic heterogeneity without limits after polymer flooding. Hence, if it is economically viable, large-size slugs are preferred.

CONCLUSIONS

Considering the flowing properties of polymer, a new parameter called "motivation coefficient" (I_P) is defined, and GC_{IP} is calculated to characterize the dynamic heterogeneity during polymer flooding. Then physical experiments and numerical simulations are done to study the variation law of GC_{IP}. The following conclusions are obtained:

(1) After the injection of polymer solution, GC_{IP} decreases to a low value in a short time, which means that the dynamic heterogeneity is greatly improved after polymer injection. However, at the subsequent water flooding stage, GC_{IP} increases sharply again and it even goes beyond that before polymer flooding, which means that the dynamic heterogeneity is more intensified when the whole polymer flooding process is over. Further enhancing oil recovery becomes more difficult after polymer flooding.

(2) Along with the increase of permeability heterogeneity, GC_{EF} decreases rapidly and SP first increases and then drops, reaching its highest value when GC_P is 0.6. Considering both SP and GCEF, 0.6 is the most favorable value of GC_P for polymer flooding.

(3) As the polymer concentration increases, GCIP reduces faster and the minimum value becomes smaller. Both S_P and GC_{EF} increase constantly as the polymer concentration rises, but the amplitude of the increase is little with the concentration beyond 0.1%. Considering both S_P and GC_{EF}, polymer concentration from 0.1% to 0.15% is the most favorable value for polymer flooding.

(4) Large-size polymer slugs extend the time during which the dynamic heterogeneity remains at a relatively low level, and hence it helps the development of low-permeability zones and enhancement of the sweep efficiency. SP increases linearly and GC_{EF} increases quickly and then slowly along with the increase of slug size. Large-size slugs are preferred if they are economically viable.

Nomenclature

Lorenz curve: It is firstly used to represent the income unbalance of the society, and then it was extended to represent the unbalance of data in industry.

Gini coefficient: It is a parameter that can be obtained from Lorenz curve and its range is from 0 to 1.

IP: The motivation coefficient, which is defined in this paper to represent dynamic heterogeneity during polymer flooding.

RP: The abbreviation of seepage resistivity. It is the reciprocal of IP.

GCIP: The Gini coefficient of IP, which is used to characterize dynamic heterogeneity in this paper.

GCP: The Gini coefficient of permeability. Similar to the classic Dykstra-Parson coefficient, it is used to characterize the heterogeneity of permeability.

SP: The area enclosed by the Gini coefficient curves of IP in polymer flooding and water flooding to evaluate the improvement of polymer injection on dynamic heterogeneity.

GCEF: It is the difference between the GCIP in the polymer and water flooding when watercut reaches 98%, to assess the final influence of polymer flooding on dynamic heterogeneity when the whole polymer flooding process is over.

ACKNOWLEDGMENT

This work was financially supported by the Indigenous Innovation Program of Qingdao City (16-5-1-46-jch), the National Natural Science Foundation of China (Grant no. 51574269), the Natural Science Foundation of Shandong Province (ZR2017QEE008), the Fundamental Research Funds for the Central Universities (Grant no. 18CX02094A; 15CX08004A), and the National Science Foundation for Distinguished Young Scholars of China (Grant No. 51625403).

REFERENCES

Alsofi, A.M. & Blunt, M.J. 2010. Streamline-based simulation of non-Newtonian polymer flooding. SPE Journal, 15 (4), 895–905.

Carrero, E., Queipo, N.V., Pintos, S. & Zerpa, L.E. 2007. Global sensitivity analysis of alkali–surfactant–polymer enhanced oil recovery processes. Journal of Petroleum Science and Engineering 58(1–2), 30–42.

Cheng, Z., Xu, R.Q., Cheng, K., Li, X.G. & Ma, L. 2010. Filtrational resistance of hydrophobic associating polymer through porous media. Special Oil and Gas Reservoir, 17(4), 91–94.

Chen, Y.H., Ye, J.G., Zhou, Y., Zhu, H.Y., Liu, T.Y. & Song, S.Y. 2015. Technology for development of high watercut oil reservoir by polymer flooding in Dagang oilfield, Oil Drilling & Production Technology, 37(3), 98–102.

Dykstra, H. & Parsons, R.L. 1950. The prediction of oil recovery by waterflood. Secondary Recovery of Oil in the United States, 160.

Gharbi, R.B. 2001. Economic optimization of EOR processes using knowledge-based system: case studies. Petroleum Science Technology, 19 (7&8), 797–823.

Hernandez, C., Chacon, L.J. & Anselmi, L. 2003. ASP system design for an offshore application in La Salina Field, Lake Maracaibo. SPE Reservoir Evaluation & Engineering 6, 147–156.

Hird, K.B. & Dubrule, O. 1998. Quantification of reservoir connectivity for reservoir description application, SPE Reservoir Evaluation and Engineering, 1, 12–17.

Khorsandi, S., Qiao, C.H. & Johns R.T. 2016. Displacement efficiency for low salinity polymer flooding including wettability alteration. Paper SPE 179695 Presented at the SPE Improved Oil Recovery Conference. Tulsa, Oklahoma, 11–13 April.

Li, A.F., Song, H.P. & Xie, H.J. 2016. Influence of inaccessible pore volume on seepage law of polymer flooding, Petroleum Geology and Recovery Efficiency 23(1), 1–6.

Liu, Y.G., Liu, H.Q., Hou, J., Wang, Q. & Dong, K. 2017. Quantitative characterization of dynamic heterogeneity in reservoirs with stratified noncommunicating layers, Journal of Energy Resources Technology 139(1), 1–11.

Lv, C.S., Guo, S.L., Zhang, X.Q. & Cui, C.Y. 2015. Polymer flooding and ASP flooding adaptability of Daqing oilfield transitional zone. Journal of Petrochemical Universities 28(6), 80–86.

Moissis D.E. & Wheeler M.F. 1990. Effect of the structure of the porous medium on unstable miscible displacement. In Dynamics of Fluids in Hierarchical Porous Media. Academic Press, San Diego, California.

Needham, R.B. & Doe, P.H. 1987. Polymer Flooding Review. SPE Journal of Petroleum Technology, 12, 1503–1507.

Niu, J.G. 2004. Practices and understanding of polymer flooding enhanced oil recovery technique in Daqing oilfield, Petroleum Geology & Oilfield Development in Daqing 23(5), 91–94.

Shi, L.T., Ye, Z.B., Zhang, Z., Zhou, C.J., Zhu S.S. & Guo Z.D. 2010. Necessity and feasibility of improving the residual resistance factor of polymer flooding in heavy oil reservoirs. Petroleum Science, 7(2), 251–256.

Shook, G.M. & Mitchell, K.M. 2009. A robust measure of heterogeneity for ranking earth models: The FPHI curve and dynamic Lorenz coefficient. Paper SPE 124625 Presented at the SPE Annual Technical Conference and Exhibition. New Orleans, Louisiana, 47- October.

Wang, D.M., Cheng, J.C., Wu, J.Z. & Wang, G. 2005. Application of polymer flooding technology in Daqing Oilfield. Acta Petrolei Sinica 26(1), 74–78.

Wang, D.M., Cheng, J.C., Yang, Q.Y., Gong, W.C., Li, Q. & Chen, F.M. 2000. Viscous-elastic polymer can increase microscale displacement efficiency in cores. Paper SPE 63227 Presented at the SPE Annual Technical Conference and Exhibition. Dallas, Texas, 14- October.

Wang, J. & Dong, M. 2009. Optimum effective viscosity of polymer solution for improving heavy oil recovery. Journal of Petroleum Science and Engineering, 67(3–4), 155–158.

Wang, X.H., Han, D.K. & Guo, S.P. 1994. Mechanism and application of polymer flooding. Acta Petrolei Sinica 15(1), 83–91.

Wu, Z.X., Shi, Z.C., Hou, X.M. & G, F. 2006. Application of resistance coefficient to optimizing parameters in polymer flooding. Petroleum Geology and Recovery Efficiency, 13(1), 92–94.

Y**ou, Y., Yue, X.A., Zhao, R.B. & Li, X.J. 2009.** Effect of chemical flooding on enhancing oil recovery after water flooding in heterogeneous reservoir, Drilling & Production Technology, 32(5), 30–33.

Submitted: 01/05/2017
Revised : 24/07/2017
Accepted : 02/08/2017

توصيف التباين الديناميكي أثناء حقن البوليمر في الخزانات ذات الطبقات غير المتصلة

يونج ليو*، ، جيان هو*،** ، جينجياو ليو *،** ، تشينج وانج *** و كاي دونج *****

* مختبر ستات كي لتصنيع النفط الثقيل، جامعة الصين للبترول، تشينغداو، شاندونغ 266580، الصين

** كلية هندسة البترول، جامعة الصين للبترول، تشينغداو، شاندونغ 266580، الصين

*** كلية هندسة البترول، جامعة الصين للبترول، بكين، الصين

**** مؤسسة بيكر هاجز، هوستين، أمريكا

الخلاصة

يؤثر التباين على الأداء التنموي بشكل كبير وبالتالي يُعتبر خاصية هامة للخزان. تعتمد الطريقة التقليدية بشكل أساسي على النفاذية والتي غالباً ما تتغير أثناء عملية الإنتاج كمعلمة لتوصيف التباين. ومع ذلك، من المرجح أن يدخل البوليمر المحقون في منطقة النفاذية العالية ذات المقاومة المنخفضة أثناء عملية الحقن مما يؤدي إلى انخفاض فرق المقاومة بين مناطق النفاذية العالية والمنخفضة. تؤدي هذه المقاومة غير المنتظمة الناتجة عن التوزيع غير المتوازن لمحلول البوليمر إلى تغيير تباين الخزان ديناميكياً والذي لا يمكن عكسه بالطريقة الحالية. في هذا البحث، تم اقتراح معلمة جديدة تسمى «معامل التحفيز» (I_P) حيث لا يتم تضمين النفاذية الثابتة فقط، بل أيضًا المعلمات الديناميكية المتعلقة بخواص البوليمر، وتم اختيار معامل جيني (GC_{IP}) لتمثيل التجانس الديناميكي خلال حقن البوليمر. تم بعد ذلك إجراء تجربة فيزيائية ومحاكاة عددية لدراسة قانون التغير في التباين الديناميكي أثناء حقن البوليمر. أظهرت النتائج تحسن كبير في التباين الديناميكي بعد حقن البوليمر. ومع ذلك، في مرحلة لاحقة لحقن الماء، كان التباين الديناميكي أكثر كثافة عندما تنتهي عملية حقن البوليمر بالكامل. مجملاً ومع الوضع في الاعتبار التنوع الديناميكي وتطور الأداء، فإن القيمة الأكثر ملاءمة لمعامل جيني للنفاذية هي 0.6، وأفضل مدى لتركيز البوليمر يتراوح من 0.1 ٪ إلى 0.15 ٪. أما بالنسبة لحجم السبيكة، يُفضل استخدام الأحجام الكبيرة إذا كانت عملية إقتصادياً.